

The spin-orbit potential and Poincaré invariance in finite temperature pNRQCD

Nora Brambilla

Physik-Department, Technische Universität München, James-Franck-Str. 1, 85748 Garching, Germany

Miguel Ángel Escobedo

Physik-Department, Technische Universität München, James-Franck-Str. 1, 85748 Garching, Germany

Jacopo Ghiglieri

Physik-Department, Technische Universität München, James-Franck-Str. 1, 85748 Garching, Germany and Excellence Cluster Universe, Technische Universität München, Boltzmannstr. 2, 85748, Garching, Germany

Antonio Vairo

Physik-Department, Technische Universität München, James-Franck-Str. 1, 85748 Garching, Germany

ABSTRACT: Heavy quarkonium at finite temperature has been the subject of intense theoretical studies, for it provides a potentially clean probe of the quark-gluon plasma. Recent studies have made use of effective field theories to exploit in a systematic manner the hierarchy of energy scales that characterize the system. In the case of a quarkonium in a medium whose temperature is smaller than the typical momentum transfer in the bound state but larger than its energy, the suitable effective field theory is pNRQCD_{HTL}, where degrees of freedom with energy or momentum larger than the binding energy have been integrated out. Thermal effects are expected to break Poincaré invariance, which, at zero temperature, manifests itself in a set of exact relations between the matching coefficients of the effective field theory. In the paper, we evaluate the leading-order thermal corrections to the spin-orbit potentials of pNRQCD_{HTL} and show that Poincaré invariance is indeed violated.

KEYWORDS: Quarkonium, finite temperature, Poincaré invariance, spin-orbit potentials.

1. Introduction

Heavy quarkonium can be systematically studied by means of non-relativistic effective field theories (EFTs) [1]. Recently, the non-relativistic EFT framework has been extended to allow the study of heavy quarkonium in a thermal bath [2, 3, 4, 5, 6, 7, 8, 9]. The relevance of heavy quarkonium, as a probe of the hot medium created by heavy ion collisions at modern accelerator machines, has been remarked since long time [10].

Heavy quarkonium is characterized by the scales typical of a non-relativistic bound state and the thermal bath is characterized by the thermodynamical scales. The former are the heavy-quark mass, m , the inverse of the typical radius of the system, $1/r$, and the binding energy, whereas the latter are the temperature T (or rather multiples of πT) and possibly smaller scales. The non-relativistic scales are hierarchically ordered: the mass is much larger than the inverse of the typical radius of the system, which in turn is much larger than the binding energy. In the weak-coupling regime, which may be relevant for the lowest quarkonium resonances [11, 12], the inverse of the typical radius of the system scales like $m\alpha_s$, while the binding energy scales like $m\alpha_s^2$. In the following, we will assume that the quarkonium is a weakly coupled bound state and that the temperature is such that

$$m \gg m\alpha_s \gg T \gg m\alpha_s^2. \quad (1.1)$$

Moreover, we will assume that all other thermodynamical scales as well as the typical hadronic scale, Λ_{QCD} , are either of the same order as or smaller than the binding energy. As it has been argued in [7, 13], this situation may be relevant for the phenomenology of the ground states of bottomonium in heavy-ion collisions at the LHC. A detailed study of the spectrum and the width of quarkonium under a more restrictive hierarchy than (1.1) can be found in [7].

One may exploit the hierarchy (1.1) by systematically integrating out degrees of freedom associated with the scales m , $m\alpha_s$ and T and by substituting QCD with low-energy EFTs better suited to describe the quarkonium in the assumed regime. It turns out that, under the scale hierarchy (1.1), quarkonium behaves like a Coulombic bound state with small thermal corrections induced by the thermal bath.

After integrating out the scales m and $m\alpha_s$ from QCD, one obtains potential Non-Relativistic QCD (pNRQCD) [14, 15]. Although in a non-relativistic EFT Poincaré invariance is not apparent, still such invariance is realized non-linearly through a set of relations among its matching coefficients [16, 17, 18, 19, 20]. One of these relations is the so-called Gromes relation [21] that relates the spin-orbit potential with the static potential.

Integrating out the temperature T from pNRQCD, one obtains pNRQCD_{HTL} [5, 22]. This EFT has the same degrees of freedom as pNRQCD, but the matching coefficients and, in particular, the potentials get thermal corrections, while the Yang–Mills Lagrangian modifies into the Hard Thermal Loop (HTL) Lagrangian [23]. Because the thermal bath introduces a preferred reference frame (the one in which the thermal bath is at rest), one expects that pNRQCD_{HTL} breaks Poincaré invariance;¹ this would have consequences

¹More precisely, the thermal bath breaks Lorentz invariance. Since, however, in the context of non-

for the properties of a heavy quarkonium moving with a certain velocity relative to the thermal bath. In order to make the statement more quantitative, we calculate in the paper the leading-order thermal contributions to the spin-orbit potential of pNRQCD_{HTL} and check them against the Gromes relation.

The paper is organized as follows. In Sec. 2, we write the pNRQCD Lagrangian and review how Poincaré invariance is realized in the effective field theory at $T = 0$. Section 3 is devoted to the computation of the leading thermal corrections to the singlet static potential and to the part of the spin-orbit potential of pNRQCD_{HTL} that depends on the centre-of-mass momentum. In Sec. 4, we show that the thermal corrections violate the Gromes relation. In Sec. 5, we calculate the leading thermal corrections to the complete spin-orbit potential and, in Sec. 6, we present our conclusions.

2. pNRQCD

The largest scale in the hierarchy (1.1) is the heavy-quark mass. Integrating it out leads to NRQCD [25, 26]. The matching is insensitive to the lower-energy scales, such as the thermal ones, therefore the EFT Lagrangian is the same as the one at zero temperature.

The next relevant scale is the inverse of the typical radius of the system, which, in the weak-coupling regime, scales like $m\alpha_s$. By integrating out this scale, we obtain weakly-coupled pNRQCD [14, 15], whose Lagrangian reads²

$$\begin{aligned} \mathcal{L}_{\text{pNRQCD}} = & \int d^3r \text{Tr} \left\{ S^\dagger (i\partial_0 - h_s) S + O^\dagger (iD_0 - h_o) O \right. \\ & - \left[(S^\dagger h_{so} O + \text{H.C.}) + \text{C.C.} \right] - \left[O^\dagger h_{oo} O + \text{C.C.} \right] \\ & \left. - \left[O^\dagger h_{oo}^A O h_{oo}^B + \text{C.C.} \right] \right\} - \frac{1}{4} F_{\mu\nu}^a F^{a\mu\nu} + \sum_{i=1}^{n_f} \bar{q}_i i\not{D} q_i. \end{aligned} \quad (2.1)$$

The fields $S = S \mathbf{1}_c / \sqrt{N_c}$ and $O = O^a T^a / \sqrt{T_F}$, are the quark-antiquark colour-singlet and colour-octet fields respectively, n_f is the number of light quark fields, q_i , $N_c = 3$ is the number of colours, $T_F = 1/2$ and $iD_0 O = i\partial_0 O - gA_0 O + O gA_0$. The trace is intended over colour and spin indices; C.C. stands for charge conjugation and H.C. stands for Hermitian conjugation. Quark-antiquark fields depend on the centre-of-mass coordinate, \mathbf{R} , on the relative distance between the quark and the antiquark, \mathbf{r} , and on time. Gluon fields depend only on \mathbf{R} and on time; this is achieved by multipole expanding them in \mathbf{r} . The operators h_s and h_o do not contain gluon fields, except for the case of h_o in covariant derivatives, and may be interpreted as the colour-singlet and the colour-octet Hamiltonians respectively; terms contributing to h_s and h_o are ordered in powers of $1/m$. The operators h_{so} , h_{oo} , h_{oo}^A and h_{oo}^B contain gluon fields; terms contributing to them are ordered in powers of $1/m$ and \mathbf{r} . We will detail these terms in the following. Since, again, the matching is insensitive to

relativistic EFTs exact relations among the matching coefficients have been derived from the Poincaré algebra [18, 19, 20], an approach that may be traced back to [24], in the paper we will keep referring to the broader Poincaré invariance.

²We adopt here and in the following the notation of [19].

the lower-energy scales, the Lagrangian (2.1) is the same as the one at zero temperature. We assume to be in the laboratory reference frame, which we define as the frame where an infinitely heavy quarkonium would be at rest.

The singlet and octet Hamiltonians read

$$h_{s,o} = \frac{\mathbf{p}^2}{m} + \frac{\mathbf{P}^2}{4m} + V_{s,o}^{(0)} + \frac{V_{s,o}^{(1)}}{m} + \frac{V_{s,o}^{(2)}}{m^2} + \dots, \quad (2.2)$$

where m is the heavy-quark mass, $\mathbf{P} = -i\mathbf{D}_{\mathbf{R}}$ and $\mathbf{p} = -i\mathbf{\nabla}_{\mathbf{r}}$. Terms in the Hamiltonian have been ordered in powers of $1/m$; the dots stand for higher-order terms. We recall that the non-relativistic power counting has $1/r \sim p \sim m\alpha_s$ and $V_{s,o}^{(0)} \sim m\alpha_s^2$, while the centre-of-mass momentum, P , may be as large as T .

The static potentials read

$$V_s^{(0)}(r) = -C_F \frac{\alpha_{V_s}}{r}, \quad V_o^{(0)}(r) = \frac{1}{2N_c} \frac{\alpha_{V_o}}{r}, \quad (2.3)$$

where $C_F = (N_c^2 - 1)/(2N_c)$ and α_{V_s} and α_{V_o} are series in α_s ; α_{V_s} is known up to three loops [27, 28], whereas α_{V_o} up to two loops [29]. At leading order, it holds that $\alpha_{V_s} = \alpha_{V_o} = \alpha_s$.

The singlet and octet propagators of pNRQCD can be expanded as

$$S^{\text{singlet}}(E) = \frac{i}{E - h_s - \Sigma_s(E) + i\eta} = \frac{i}{E - h_s + i\eta} + \frac{i}{E - h_s + i\eta} \Sigma_s(E) \frac{1}{E - h_s + i\eta} + \dots, \quad (2.4)$$

$$S_{ab}^{\text{octet}}(E) = \left(\frac{i}{E - h_o - \Sigma_o(E) + i\eta} \right)_{ab} = \frac{i\delta_{ab}}{E - h_o + i\eta} + \frac{i}{E - h_o + i\eta} \Sigma_o(E)_{ab} \frac{1}{E - h_o + i\eta} + \dots, \quad (2.5)$$

where $\Sigma_{s,o}$ are the colour-singlet and colour-octet self-energies. According to the power counting of pNRQCD and the fact that $V_{s,o}^{(1)} \sim V_{s,o}^{(2)} \ll m\alpha_s^2$, the propagator $1/(E - h_{s,o} + i\eta)$ may, in turn, be expanded as

$$\frac{1}{E - h_{s,o} + i\eta} = \frac{1}{E - h_{s,o}^{(0)} + i\eta} + \frac{1}{E - h_{s,o}^{(0)} + i\eta} \left[\frac{\mathbf{P}^2}{4m} + \frac{V_{s,o}^{(1)}}{m} + \frac{V_{s,o}^{(2)}}{m^2} + \dots \right] \frac{1}{E - h_{s,o}^{(0)} + i\eta} + \dots, \quad (2.6)$$

where $h_s^{(0)} = \frac{\mathbf{p}^2}{m} - C_F \frac{\alpha_s}{r}$ and $h_o^{(0)} = \frac{\mathbf{p}^2}{m} + \frac{1}{2N_c} \frac{\alpha_s}{r}$ are the leading-order singlet and octet Hamiltonians respectively.

The explicit form of the non-static potentials $V_s^{(1)}$ and $V_s^{(2)}$ can be read from [30, 1]. In particular, we will concern ourselves with the colour-singlet, V_{LSs} , and the colour octet, V_{LSo} , spin-orbit potentials, which are part of $V_s^{(2)}$ and $V_o^{(2)}$ respectively. They can be conveniently split into a part that depends on the centre-of-mass momentum \mathbf{P} and a part

that depends on the relative momentum \mathbf{p} :

$$V_{LSs} = \frac{(\mathbf{r} \times \mathbf{P}) \cdot (\boldsymbol{\sigma}^{(1)} - \boldsymbol{\sigma}^{(2)})}{4m^2} V_{LSsa}(r) + \frac{(\mathbf{r} \times \mathbf{p}) \cdot (\boldsymbol{\sigma}^{(1)} + \boldsymbol{\sigma}^{(2)})}{2m^2} V_{LSsb}(r), \quad (2.7)$$

$$V_{LSo} = \frac{(\mathbf{r} \times \mathbf{P}) \cdot (\boldsymbol{\sigma}^{(1)} - \boldsymbol{\sigma}^{(2)})}{4m^2} V_{LSoa}(r) + \frac{(\mathbf{r} \times \mathbf{p}) \cdot (\boldsymbol{\sigma}^{(1)} + \boldsymbol{\sigma}^{(2)})}{2m^2} V_{LSob}(r), \quad (2.8)$$

where the Pauli matrices $\boldsymbol{\sigma}^{(1)}$ and $\boldsymbol{\sigma}^{(2)}$ act on the heavy quark and antiquark respectively. At leading order, it holds that

$$V_{LSsa}(r) = -\frac{C_F \alpha_s}{2 r^3}, \quad V_{LSsb}(r) = \frac{3C_F \alpha_s}{2 r^3}, \quad V_{LSoa}(r) = \frac{1}{4N_c} \frac{\alpha_s}{r^3}, \quad V_{LSob}(r) = -\frac{3}{4N_c} \frac{\alpha_s}{r^3}, \quad (2.9)$$

which implies that $V_{LSsa} \sim V_{LSsb} \sim V_{LSoa} \sim V_{LSob} \sim m^3 \alpha_s^4$.

The matching coefficients, and among them the potentials, that appear in the pNRQCD Lagrangian obey a set of relations due to Poincaré invariance [19]. For the kinetic terms in Eq. (2.2), such relations impose that the coefficient of the operator $\mathbf{P}^2/(4m)$ is one, which also implies that the coefficient of the operator \mathbf{p}^2/m is one. Among the relations fulfilled by the potentials, there are some exact relations linking the spin-orbit potentials V_{LSsa} and V_{LSoa} to the static potentials:

$$V_{LSsa}(r) = -\frac{V_s^{(0)}(r)'}{2r}, \quad V_{LSoa}(r) = -\frac{V_o^{(0)}(r)'}{2r}, \quad (2.10)$$

where $f(r)' \equiv df(r)/dr$. The first relation is known as the Gromes relation, because it was first derived in [21] from the transformation properties of some Wilson loops under Lorentz boosts (see also [18]).

In the next section, we will compute the leading thermal correction to the spin-orbit potential V_{LSsa} by matching to pNRQCD_{HTL}. To this end we will need some of the terms appearing in the operator h_{so} of the pNRQCD Lagrangian (2.1). These may be ordered in powers of $1/m$ and \mathbf{r} as

$$h_{so} = h_{so}^{(0,1)} + h_{so}^{(0,2)} + h_{so}^{(1,0)} + h_{so}^{(1,1)} + h_{so}^{(2,0)} + \dots, \quad (2.11)$$

where the indices (i, j) refer to the order in powers of $1/m$ and \mathbf{r} respectively. The dots stand for higher-orders terms. The explicit expressions of $h_{so}^{(i,j)}$ may be taken from [19] and read

$$h_{so}^{(0,1)} = -\frac{V_{so}^{(0,1)}(r)}{2} \mathbf{r} \cdot g\mathbf{E}, \quad (2.12)$$

$$h_{so}^{(1,0)} = -\frac{c_F}{2m} V_{sob}^{(1,0)}(r) \boldsymbol{\sigma}^{(1)} \cdot g\mathbf{B} - \frac{1}{2m} \frac{V_{soc}^{(1,0)}(r)}{r^2} (\mathbf{r} \cdot \boldsymbol{\sigma}^{(1)}) (\mathbf{r} \cdot g\mathbf{B}) - \frac{1}{m} \frac{V_{sod}^{(1,0)}(r)}{2r} \mathbf{r} \cdot g\mathbf{E}, \quad (2.13)$$

$$h_{so}^{(1,1)} = \frac{1}{8m} V_{so}^{(1,1)}(r) \{\mathbf{P} \cdot, \mathbf{r} \times g\mathbf{B}\} + \dots, \quad (2.14)$$

$$\begin{aligned}
h_{so}^{(2,0)} &= \frac{c_s}{16m^2} V_{soa}^{(2,0)}(r) \boldsymbol{\sigma}^{(1)} \cdot [\mathbf{P} \times, g\mathbf{E}] \\
&+ \frac{1}{16m^2} \frac{V_{sob'}^{(2,0)}(r)}{r^2} (\mathbf{r} \cdot \boldsymbol{\sigma}^{(1)}) \{ \mathbf{P} \cdot, (g\mathbf{E} \times \mathbf{r}) \} \\
&+ \frac{1}{16m^2} \frac{V_{sob''}^{(2,0)}(r)}{r^2} \{ (\mathbf{r} \cdot g\mathbf{E}), \mathbf{P} \cdot (\mathbf{r} \times \boldsymbol{\sigma}^{(1)}) \} \\
&+ \frac{1}{16m^2} \frac{V_{sob'''}^{(2,0)}(r)}{r^2} \{ (\mathbf{r} \cdot \mathbf{P}), \boldsymbol{\sigma}^{(1)} \cdot (\mathbf{r} \times g\mathbf{E}) \} \\
&+ \frac{1}{8m^2} \frac{V_{soe}^{(2,0)}(r)}{r} \{ \mathbf{P} \cdot, \mathbf{r} \times g\mathbf{B} \} + \dots .
\end{aligned} \tag{2.15}$$

Charge conjugation invariance requires that $h_{so}^{(0,2)} = 0$. The field \mathbf{E} is the chromoelectric field, $E^i = F^{i0}$, the field \mathbf{B} is the chromomagnetic field, $B^i = -\varepsilon_{ijk} F^{jk}/2$, $[\mathbf{P} \times, g\mathbf{E}] = \mathbf{P} \times g\mathbf{E} - g\mathbf{E} \times \mathbf{P}$ and similarly for the anticommutators. For $h_{so}^{(1,1)}$ and $h_{so}^{(2,0)}$ only the \mathbf{P} -dependent terms have been displayed. The coefficients c_F and c_s are inherited from NRQCD and encode non-analytical contributions in $1/m$, whereas the various $V_{so}^{(i,j)}(r)$ come from the matching to pNRQCD and encode non-analytical contributions in r . At leading order in the coupling, the matching gives $c_F = c_s = 1$ and $V_{so}^{(0,1)}(r) = V_{sob}^{(1,0)}(r) = V_{soa}^{(2,0)}(r) = V_{so}^{(1,1)}(r) = 1$, while all other matching coefficients are of order α_s or smaller.

Poincaré invariance imposes further constraints on the matching coefficients. For instance, at the NRQCD level, we have that $2c_F - c_s - 1 = 0$ to all orders [16, 17]. At the level of pNRQCD, the following exact relations hold [19]

$$V_{so}^{(1,1)}(r) = V_{so}^{(0,1)}(r), \tag{2.16}$$

$$2c_F V_{sob}^{(1,0)}(r) - c_s V_{soa}^{(2,0)}(r) = V_{so}^{(0,1)}(r), \tag{2.17}$$

$$2c_F V_{sob}^{(1,0)}(r) - c_s V_{soa}^{(2,0)}(r) - V_{sob''}^{(2,0)}(r) = \left(r V_{so}^{(0,1)}(r) \right)'. \tag{2.18}$$

Combining the last two it follows that

$$V_{sob''}^{(2,0)}(r) = -r V_{so}^{(0,1)}(r)'. \tag{2.19}$$

An interesting consequence of this relation is that, since $V_{so}^{(0,1)}(r)$ is at least of order α_s^2 [31] but has not infrared divergences at that order [32], $V_{sob''}^{(2,0)}(r)$ is at least of order α_s^3 .

3. pNRQCD_{HTL}

In this section, we compute the leading temperature-dependent correction to the colour-singlet static potential, $V_s^{(0)}$, and spin-orbit potential, V_{LSsa} , which amounts to matching the colour-singlet static and spin-orbit potentials in the EFT that follows from pNRQCD after integrating out the temperature. This EFT is called pNRQCD_{HTL} [5, 6, 22]. Its Lagrangian reads

$$\begin{aligned}
\mathcal{L}_{\text{pNRQCD}_{\text{HTL}}} &= \int d^3r \text{Tr} \left\{ \mathbf{S}^\dagger [i\partial_0 - h_s - \delta V_s] \mathbf{S} + \mathbf{O}^\dagger [iD_0 - h_o - \delta V_o] \mathbf{O} \right\} \\
&+ \mathcal{L}_{\text{HTL}} + \dots,
\end{aligned} \tag{3.1}$$

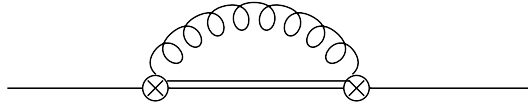


Figure 1: The leading heavy quarkonium self-energy diagram. Single lines stand for leading-order quark-antiquark colour-singlet propagators, $i/(E - h_s^{(0)} + i\eta)$, double lines for leading-order quark-antiquark colour-octet propagators, $i\delta_{ab}/(E - h_o^{(0)} + i\eta)$, curly lines for gluons and the vertices are the chromoelectric dipole vertices induced by $h_{so}^{(0,1)}$.

where δV_s and δV_o are the thermal corrections to the colour-singlet and colour-octet potentials respectively, \mathcal{L}_{HTL} is the HTL Lagrangian for the gauge and light-quark degrees of freedom [23] and the dots stand for singlet-octet and octet-octet operators suppressed by powers of $1/m$ and \mathbf{r} , whose computation is beyond the scope of the paper.

The terms δV_s and δV_o encode the corrections to the potentials induced by the thermal bath. They are evaluated by matching real-time propagators in pNRQCD with the corresponding expressions in pNRQCD_{HTL}. It has been pointed out in [5, 7] that the doubling of degrees of freedom, typical of the real-time formalism, does not affect heavy quarks for which the unphysical degrees of freedom decouple. Hence, in the following, we will only deal with the physical singlet and octet propagators, which have been written in Eqs. (2.4) and (2.5) respectively. The matching may be done perturbatively, because we have assumed $T \gg \Lambda_{\text{QCD}}$; contributions coming from other thermal scales do not affect the potentials, because we have assumed that the other thermal scales are at most as large as the binding energy. More specifically, the pNRQCD singlet propagator (2.4) is matched to the pNRQCD_{HTL} expression

$$Z_s^{1/2} \frac{i}{E - h_s - \delta V_s + i\eta} Z_s^{1/2\dagger} = \frac{i}{E - h_s + i\eta} + \frac{i}{E - h_s + i\eta} \delta V_s \frac{1}{E - h_s + i\eta} + \left\{ \delta Z_s, \frac{i}{E - h_s + i\eta} \right\} + \dots \quad (3.2)$$

There is no self-energy contribution in (3.2), because this would correspond to a scaleless integral eventually irrelevant (e.g. in dimensional regularization it would vanish). $Z_s^{1/2} = 1 + \delta Z_s$ is the normalization of the singlet field in pNRQCD_{HTL}; δZ_s is of order α_s and a function of \mathbf{r} , which implies that it does not commute with h_s . At our accuracy, δZ_s is real.

We will assume the thermal bath to be a quark-gluon plasma at rest with respect to the laboratory reference frame. This implies, in particular, that the Bose–Einstein distribution,

$$n_{\text{B}}(x) = \frac{1}{e^{x/T} - 1}, \quad (3.3)$$

which describes the distribution of the gluons in the bath, depends only on their energy.

3.1 Singlet static potential in pNRQCD_{HTL}

We start by evaluating the leading thermal correction of the static potential, $\delta V_s^{(0)}$, which was first done in [5], and the leading thermal correction of δZ_s , which is new. These

corrections originate from the pNRQCD diagram shown in Fig. 1, whose contribution to $\Sigma_s(E)$ reads

$$\begin{aligned} \Sigma_s(E)^{\text{Fig. 1}} = & -iC_F g^2 \left(V_{so}^{(0,1)}(r) \right)^2 \frac{2}{3} r^i \int \frac{d^4 k}{(2\pi)^4} \frac{i}{E - h_o^{(0)} - k_0 + i\eta} k_0^2 \\ & \times \left[\frac{i}{k_0^2 - k^2 + i\eta} + 2\pi\delta(k_0^2 - k^2) n_B(|k_0|) \right] r^i, \end{aligned} \quad (3.4)$$

where k is the modulus of the three-momentum \mathbf{k} . Evaluating the integral over the momentum region $k_0, k \sim T \gg (E - h_o^{(0)})$ implies that we may expand

$$\frac{i}{E - h_o^{(0)} - k_0 + i\eta} = \frac{i}{-k_0 + i\eta} - i \frac{E - h_o^{(0)}}{(-k_0 + i\eta)^2} + i \frac{(E - h_o^{(0)})^2}{(-k_0 + i\eta)^3} + \dots \quad (3.5)$$

It is convenient then to regularize the integral in dimensional regularization, because the non-thermal part, which is scaleless, vanishes, and we are left with the thermal part only, which is finite. The leading contribution comes from the term in (3.5) that is linear in $E - h_o^{(0)}$; after performing the integration, it reads

$$\Sigma_s(E)^{\text{Fig. 1}} = -\frac{2\pi}{9} C_F \alpha_s \left(V_{so}^{(0,1)}(r) \right)^2 T^2 r^i (E - h_o^{(0)}) r^i. \quad (3.6)$$

A useful identity is

$$r^i (E - h_o^{(0)}) r^i = \frac{1}{2} \left[[r^i, E - h_s^{(0)}], r^i \right] + \frac{1}{2} \{ r^2, E - h_s^{(0)} \} - (V_o^{(0)} - V_s^{(0)}) r^2, \quad (3.7)$$

which follows from $h_o^{(0)} = h_s^{(0)} + (h_o^{(0)} - h_s^{(0)}) = h_s^{(0)} + (V_o^{(0)} - V_s^{(0)})$. The identity is useful, because the first term in the right-hand side is of order $1/m$ and, therefore, does not contribute to the static potential, the second term contributes only to the singlet normalization, Z_s , and the third term to the static potential. Substituting (3.7) into (3.6) and then matching (2.4) to (3.2) gives the leading-order thermal corrections to the static potential and the singlet normalization:

$$\delta V_s^{(0)}(r) = \frac{2\pi}{9} C_F \alpha_s \left(V_{so}^{(0,1)}(r) \right)^2 T^2 r^2 (V_o^{(0)}(r) - V_s^{(0)}(r)), \quad (3.8)$$

$$\delta Z_s(r) = -\frac{\pi}{9} C_F \alpha_s \left(V_{so}^{(0,1)}(r) \right)^2 T^2 r^2, \quad (3.9)$$

where $V_o^{(0)}(r) - V_s^{(0)}(r) = N_c \alpha_s / (2r)$. The power counting of pNRQCD and Eq. (1.1) give the size of $\delta V_s^{(0)}$: $m\alpha_s^3 \gg \delta V_s^{(0)} \sim \alpha_s^2 T^2 r \gg m\alpha_s^5$. We recall that at higher orders $\delta V_s^{(0)}$ develops also an imaginary part [5] (see also [2]).

3.2 Singlet spin-orbit potential $\delta V_{LS\,sa}$ in pNRQCD_{HTL}

In [7], all contributions to δV_s , static and non-static, that contribute to the spectrum up to order $m\alpha_s^5$ were computed. Up to that order, no spin-dependent corrections are relevant. The aim of this section is to compute the leading spin-orbit terms in δV_s . In particular,

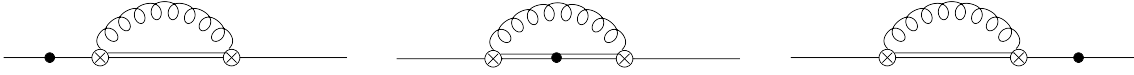


Figure 2: Diagrams contributing to $\delta V_{LS,a}$. The dot stands for an insertion of the spin-orbit potential proportional to $V_{LS sa}$ (left and right diagram) or to $V_{LS oa}$ (middle diagram), all other symbols are as in Fig. 1.

we will compute the leading thermal correction, $\delta V_{LS sa}$, to the centre-of-mass momentum dependent spin-orbit potential $V_{LS sa}$, defined in Eq. (2.7). The computation follows the same line as the one for $\delta V_s^{(0)}$: we calculate thermal spin-dependent corrections to the pNRQCD singlet propagator, and match it to the singlet propagator in pNRQCD_{HTL}.

We identify the following set of contributions to $\delta V_{LS sa}$:

$$\delta V_{LS sa} = \delta V_{LS,a} + \delta V_{LS,b} + \delta V_{LS,c} + \delta V_{LS,d} + \delta V_{LS,e}, \quad (3.10)$$

where

- (1) $\delta V_{LS,a}$ comes from inserting a spin-orbit potential in the singlet or octet propagators of the diagram in Fig. 1;
- (2) $\delta V_{LS,b}$ comes from replacing one of the two chromoelectric dipole vertices in Fig. 1 with the chromomagnetic vertex proportional to $c_F V_{sob}^{(1,0)}$ in Eq. (2.13) and inserting a centre-of-mass kinetic energy into the octet propagator;
- (3) $\delta V_{LS,c}$ comes from replacing one of the chromoelectric dipole vertices in Fig. 1 with the vertex proportional to $c_s V_{soa}^{(2,0)}$ in Eq. (2.15);
- (4) $\delta V_{LS,d}$ comes from replacing one of the chromoelectric dipole vertices in Fig. 1 with the vertex proportional to $V_{sob''}^{(2,0)}$ in Eq. (2.15);
- (5) $\delta V_{LS,e}$ comes from replacing one of the chromoelectric dipole vertices in Fig. 1 with the vertex proportional to $c_F V_{sob}^{(1,0)}$ in Eq. (2.13) and the other one with the vertex given by $h_{so}^{(1,1)}$ in Eq. (2.14).

By explicit inspection, one sees that diagrams with vertices given by the terms proportional to $V_{soc}^{(1,0)}$, $V_{sob'}^{(2,0)}$ and $V_{sob''}^{(2,0)}(r)$ in Eqs. (2.13) and (2.15), albeit spin-dependent, do not contribute to the spin-orbit potential.

3.2.1 Evaluation of $\delta V_{LS,a}$

We evaluate the diagrams in Fig. 2. As in the previous calculation of the thermal correction to the static propagator, we expand the octet propagators for $k_0 \gg E - h_o^{(0)}$ (see Eq. (3.5)). The leading contribution comes again from the linear term that we treat by means of the

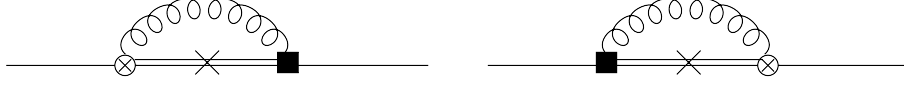


Figure 3: Diagrams contributing to $\delta V_{LS,b}$. The square stands for the chromomagnetic vertex proportional to $c_F V_{sob}^{(1,0)}(r)$, the cross for a centre-of-mass kinetic energy insertion, and all other symbols are as in Fig. 1.

identity (3.7). The left diagram of Fig. 2 gives

$$-\frac{2\pi}{9} C_F \alpha_s T^2 \frac{i}{E - h_s^{(0)}} \left(V_{so}^{(0,1)}(r) \right)^2 \left[\frac{1}{2} \left\{ r^2, E - h_s^{(0)} \right\} - \left(V_o^{(0)}(r) - V_s^{(0)}(r) \right) r^2 \right] \\ \times \frac{1}{E - h_s^{(0)}} \frac{(\mathbf{r} \times \mathbf{P}) \cdot (\boldsymbol{\sigma}^{(1)} - \boldsymbol{\sigma}^{(2)})}{4m^2} V_{LS\ sa}(r) \frac{1}{E - h_s^{(0)}}, \quad (3.11)$$

the right one gives

$$-\frac{2\pi}{9} C_F \alpha_s T^2 \frac{i}{E - h_s^{(0)}} \frac{(\mathbf{r} \times \mathbf{P}) \cdot (\boldsymbol{\sigma}^{(1)} - \boldsymbol{\sigma}^{(2)})}{4m^2} V_{LS\ sa}(r) \frac{1}{E - h_s^{(0)}} \\ \times \left(V_{so}^{(0,1)}(r) \right)^2 \left[\frac{1}{2} \left\{ r^2, E - h_s^{(0)} \right\} - \left(V_o^{(0)}(r) - V_s^{(0)}(r) \right) r^2 \right] \frac{1}{E - h_s^{(0)}}, \quad (3.12)$$

and the middle one gives

$$\frac{2\pi}{9} C_F \alpha_s T^2 \frac{i}{E - h_s^{(0)}} \left(V_{so}^{(0,1)}(r) \right)^2 r^2 \frac{(\mathbf{r} \times \mathbf{P}) \cdot (\boldsymbol{\sigma}^{(1)} - \boldsymbol{\sigma}^{(2)})}{4m^2} V_{LS\ oa}(r) \frac{1}{E - h_s^{(0)}}, \quad (3.13)$$

where we have kept only terms relevant at order $1/m^2$. Matching to the pNRQCD_{HTL} propagator (3.2), expanded according to (2.6), we observe that the terms proportional to $(V_o^{(0)} - V_s^{(0)})r^2$ in (3.11) and (3.12) cancel against one insertion of $\delta V_s^{(0)}(r)$ and one of the spin-orbit potential in the pNRQCD_{HTL} propagator, while the term proportional to $(E - h_s^{(0)})r^2/2$ in (3.11) and the one proportional to $r^2(E - h_s^{(0)})/2$ in (3.12) cancel against the term $\left\{ \delta Z_s, i/(E - h_s^{(0)}) \times [\text{spin-orbit potential}] \times 1/(E - h_s^{(0)}) \right\}$ in (3.2). The expression of δZ_s can be read from Eq. (3.9). What is left gives the leading-order thermal correction, coming from the diagrams in Fig. 2, to the centre-of-mass momentum dependent spin-orbit potential:

$$\delta V_{LS,a}(r) = \frac{2\pi}{9} C_F \alpha_s \left(V_{so}^{(0,1)}(r) \right)^2 T^2 r^2 (V_{LS\ oa}(r) - V_{LS\ sa}(r)). \quad (3.14)$$

According to the power counting of pNRQCD and Eq. (1.1), we have that $m\alpha_s^5 \gg \delta V_{LS,a}(\mathbf{r} \times \mathbf{P}) \cdot (\boldsymbol{\sigma}^{(1)} - \boldsymbol{\sigma}^{(2)})/m^2 \gg m\alpha_s^8$.

3.2.2 Evaluation of $\delta V_{LS,b}$

We evaluate the diagrams in Fig. 3. Their thermal contribution to $\Sigma_s(E)$ reads

$$\begin{aligned} \Sigma_s(E)^{\text{Fig. 3}} &= -2ig^2 C_F V_{so}^{(0,1)}(r) V_{sob}^{(1,0)}(r) \frac{c_F}{2m} \\ &\times r^i \int \frac{d^4 k}{(2\pi)^4} \frac{i}{E - h_o^{(0)} - k_0 + i\eta} \frac{(\mathbf{P} - \mathbf{k})^2}{4m} \frac{1}{E - h_o^{(0)} - k_0 + i\eta} \\ &\times k_0 \epsilon^{jln} k^l \left(\delta^{ni} - \frac{k^n k^i}{k^2} \right) 2\pi \delta(k_0^2 - k^2) n_B(|k_0|) (\sigma^{(1)j} - \sigma^{(2)j}), \end{aligned} \quad (3.15)$$

while the non-thermal part vanishes if regularized in dimensional regularization. The factor 2 follows from the fact that the two diagrams give the same contribution at order $1/m^2$. The octet propagators may be expanded according to Eq. (3.5); considering that, besides the two octet propagators, the integral in (3.15) is odd in k_0 , the leading non-vanishing term coming from their expansion is $-2(E - h_o^{(0)})/(-k_0 + i\eta)^3$. The factor $E - h_o^{(0)}$ contains a part, $E - h_s^{(0)}$, that contributes to the singlet normalization, and a part, $V_s^{(0)} - V_o^{(0)}$, that contributes to the spin-orbit potential. The octet centre-of-mass kinetic energy, $(\mathbf{P} - \mathbf{k})^2/(4m)$, contributes to the spin-orbit potential only through the term $-\mathbf{P} \cdot \mathbf{k}/(2m)$. With this in mind, we match (2.4) to (3.2) and obtain the leading-order thermal correction, coming from the diagrams in Fig. 3, to the centre-of-mass momentum dependent spin-orbit potential:

$$\delta V_{LS,b}(r) = -\frac{4\pi}{9} C_F \alpha_s c_F V_{so}^{(0,1)}(r) V_{sob}^{(1,0)}(r) T^2 \left(V_o^{(0)}(r) - V_s^{(0)}(r) \right). \quad (3.16)$$

Considering that the matching coefficients c_F , $V_{so}^{(0,1)}$ and $V_{sob}^{(1,0)}$ are one at leading order, the size of the correction is $m\alpha_s^5 \gg \delta V_{LS,b}(\mathbf{r} \times \mathbf{P}) \cdot (\boldsymbol{\sigma}^{(1)} - \boldsymbol{\sigma}^{(2)})/m^2 \gg m\alpha_s^8$.

3.2.3 Evaluation of $\delta V_{LS,c}$

The calculation of $\delta V_{LS,c}$ is at this point simple: there are two contributing diagrams, which may be constructed by replacing one of the chromoelectric dipole vertices in Fig. 1 with the vertex proportional to $c_s V_{soa}^{(2,0)}$ in Eq. (2.15). Since this vertex contains a chromoelectric field as well, the integration is exactly the same as the one performed in Eq. (3.4). The only change is in the prefactor of the integral. Matching to the pNRQCD_{HTL} propagator, we obtain at leading order

$$\delta V_{LS,c}(r) = \frac{2\pi}{9} C_F \alpha_s c_s V_{so}^{(0,1)}(r) V_{soa}^{(2,0)}(r) T^2 \left(V_o^{(0)}(r) - V_s^{(0)}(r) \right), \quad (3.17)$$

which, considering that c_s , $V_{so}^{(0,1)}$ and $V_{soa}^{(2,0)}$ are one at leading order, has the same size as $\delta V_{LS,b}$.

3.2.4 Evaluation of $\delta V_{LS,d}$

The calculation of $\delta V_{LS,d}$ is similar to this last one, but with the vertices proportional to $c_s V_{soa}^{(2,0)}$ replaced by the ones proportional to $V_{sob''}^{(2,0)}$ in Eq. (2.15). The leading-order result reads

$$\delta V_{LS,d}(r) = \frac{2\pi}{9} C_F \alpha_s V_{so}^{(0,1)}(r) V_{sob''}^{(2,0)}(r) T^2 \left(V_o^{(0)}(r) - V_s^{(0)}(r) \right). \quad (3.18)$$

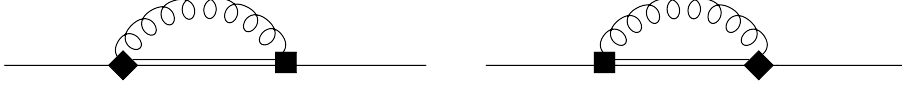


Figure 4: Diagrams contributing to $\delta V_{LS,e}$. The diamond stands for the vertex $h_{so}^{(1,1)}$, given in Eq. (2.14), and all other symbols are as in Fig. 3.

Considering that $V_{so}^{(0,1)}$ is one at leading order, but that $V_{sob'}^{(2,0)}$ is at least of order α_s^3 , $\delta V_{LS,d}(r)$ is suppressed with respect to $\delta V_{LS,a}$, $\delta V_{LS,b}$ and $\delta V_{LS,c}$ by, at least, a factor α_s^3 .

3.2.5 Evaluation of $\delta V_{LS,e}$

We evaluate the diagrams in Fig. 4. Their thermal contribution to $\Sigma_s(E)$ reads

$$\begin{aligned} \Sigma_s(E)^{\text{Fig. 4}} &= -2ig^2 C_F V_{so}^{(1,1)}(r) V_{sob}^{(1,0)}(r) \frac{c_F}{2m} \left(-\frac{(\mathbf{P} \times \mathbf{r})^i}{2m} \right) \int \frac{d^4k}{(2\pi)^4} \frac{i}{E - h_o^{(0)} - k_0 + i\eta} \\ &\quad \times (ik^l) e^{jlr} e^{ins} (-ik^n) \left(\delta^{rs} - \frac{k^r k^s}{k^2} \right) 2\pi \delta(k_0^2 - k^2) n_B(|k_0|) (\sigma^{(1)j} - \sigma^{(2)j}), \end{aligned} \quad (3.19)$$

while the non-thermal part vanishes if regularized in dimensional regularization. The factor 2 follows from the fact that the two diagrams give the same contribution at order $1/m^2$. The octet propagators may be expanded according to Eq. (3.5): the linear term in $E - h_o^{(0)}$ contains a part, $E - h_s^{(0)}$, that contributes to the singlet normalization, and a part, $V_s^{(0)} - V_o^{(0)}$, that contributes to the spin-orbit potential. This last contribution reads

$$\delta V_{LS,e}(r) = \frac{4\pi}{9} C_F \alpha_s c_F V_{so}^{(1,1)}(r) V_{sob}^{(1,0)}(r) T^2 \left(V_o^{(0)}(r) - V_s^{(0)}(r) \right). \quad (3.20)$$

Considering that, according to (2.16), the matching coefficient $V_{so}^{(1,1)}$ is equal to $V_{so}^{(0,1)}$, $\delta V_{LS,e}$ exactly cancels with $\delta V_{LS,b}$ in the sum (3.10).

3.2.6 Summary

In summary, the leading thermal correction to the centre-of-mass momentum-dependent spin-orbit potential,

$$\delta V_{LSs} |_{\mathbf{P}\text{-dependent}} = \frac{(\mathbf{r} \times \mathbf{P}) \cdot (\boldsymbol{\sigma}^{(1)} - \boldsymbol{\sigma}^{(2)})}{4m^2} \delta V_{LSsa}(r), \quad (3.21)$$

is the sum of Eqs. (3.14), (3.16), (3.17), (3.18) and (3.20); it reads:

$$\begin{aligned} \delta V_{LSsa}(r) &= \frac{2\pi}{9} C_F \alpha_s V_{so}^{(0,1)}(r) T^2 \left\{ V_{so}^{(0,1)}(r) r^2 (V_{LSoa}(r) - V_{LSsa}(r)) \right. \\ &\quad \left. + \left[c_s V_{soa}^{(2,0)}(r) + V_{sob'}^{(2,0)}(r) \right] \left(V_o^{(0)}(r) - V_s^{(0)}(r) \right) \right\} \\ &= \frac{\pi}{6} C_F N_c \frac{\alpha_s^2}{r} T^2 + \text{higher orders}. \end{aligned} \quad (3.22)$$

In the first equality of (3.22), the matching coefficients of NRQCD and pNRQCD have been kept unexpanded; this amounts at having provided an expression for the spin-orbit

potential that resums contributions from the scales m and $m\alpha_s$, while it is of leading order in the temperature. In the second equality, we have kept only the leading terms in the NRQCD and pNRQCD matching coefficients. We note that the contribution coming from the term proportional to $V_{sob''}^{(2,0)}$ is negligible, of the same size or smaller than subleading thermal corrections that we have neglected throughout the paper.

4. Gromes relation at finite temperature

After having computed the leading contributions to $\delta V_{LS\ sa}$, we can now check whether these new terms fulfill the Gromes relation (2.10) or not. This corresponds to verifying the equality

$$\delta V_{LS\ sa}(r) \stackrel{?}{=} -\frac{\delta V_s^{(0)}(r)'}{2r}. \quad (4.1)$$

We use the expression of $\delta V_{LS\ sa}$ provided by the first equality in Eq. (3.22) that keeps unexpanded the matching coefficients of NRQCD and pNRQCD. If we make use of the relations (2.10) and (2.19), which are exact, then $\delta V_{LS\ sa}$ may be rewritten as

$$\begin{aligned} \delta V_{LS\ sa}(r) = & -\frac{\delta V_s^{(0)}(r)'}{2r} \\ & + \frac{2\pi}{9} C_F \alpha_s V_{so}^{(0,1)}(r) T^2 \left(c_s V_{soa}^{(2,0)}(r) + V_{so}^{(0,1)}(r) \right) \left(V_o^{(0)}(r) - V_s^{(0)}(r) \right), \end{aligned} \quad (4.2)$$

which shows that the Gromes relation is violated by an amount, which at leading order is $\frac{2\pi}{9} C_F N_c \frac{\alpha_s^2}{r} T^2$.

4.1 The spin-orbit potential in a covariant model

In order to understand the origin of the observed violation of Poincaré invariance, it is useful to consider at zero temperature the case of a massive gluon, whose mass, m_g , is such that $m\alpha_s \gg m_g \gg m\alpha_s^2$. The massive gluon contributes to the potential, but clearly it does not break Poincaré invariance. To see this let us evaluate the corrections to the spin-orbit potential. The diagrams contributing to the spin-orbit potential are the same of those considered in the previous section, only now the gluon propagator reads (in the unitary gauge)

$$-\frac{i}{k_0^2 - k^2 - m_g^2 + i\eta} \left(g_{\mu\nu} - \frac{k_\mu k_\nu}{m_g^2} \right). \quad (4.3)$$

The contributions to the static potential, $\delta V_s^{(0)}$, and $\delta V_{LS,a}$, $\delta V_{LS,c}$ and $\delta V_{LS,d}$ depend on the correlator of two chromoelectric fields. They are proportional to

$$\int \frac{d^d k}{(2\pi)^d} \frac{i}{E - h_o^{(0)} - k_0 + i\eta} \frac{1}{k_0^2 - k^2 - m_g^2 + i\eta} [(d-1)k_0^2 - k^2], \quad (4.4)$$

where we have regularized the integral in dimensional regularization. Integrating over the momentum region $k_0, k \sim m_g$ means that we are expanding the octet propagator according to Eq. (3.5). We will focus here only on the term linear in $E - h_o^{(0)}$, since this is the relevant

term in the finite temperature case analyzed in the rest of the paper.³ It turns out that the linear term vanishes in dimensional regularization (see [15]). The reason is that the contribution coming from the spatial components of the gluon propagator (proportional to $(d-1)k_0^2$ in the equation) cancels against the contribution coming from the temporal component (proportional to k^2 in the equation). This is in sharp contrast with the finite temperature case, where the term linear in $E - h_o^{(0)}$ does not vanish (in Coulomb gauge, this is due to the fact that only the spatial components of the gluon propagator get thermal contributions) and eventually generate a finite thermal contribution to $\delta V_s^{(0)}$, $\delta V_{LS,a}$, $\delta V_{LS,c}$ and $\delta V_{LS,d}$ (see Eqs. (3.8), (3.14), (3.17) and (3.18) respectively).

The contributions to $\delta V_{LS,b}$ and $\delta V_{LS,e}$ depend on the spatial components of the gluon propagator only. Both $\delta V_{LS,b}$ and $\delta V_{LS,e}$ get finite contributions from the massive gluon but the sum of the two terms linear in $E - h_o^{(0)}$ vanishes: the same happens in the finite temperature case discussed in the previous section.

The massive gluon example provides a simple case where Poincaré invariance is not broken. The Gromes relation is trivially realized for terms that are linear in the energy: such terms vanish for both the static and the spin-orbit potentials. In the finite temperature case, diagrams that depend on the correlator of two chromoelectric fields, like the one shown in Fig. 1, do not vanish. This is a direct consequence of the fact that the thermal bath affects in a non-covariant way the gluon propagator.

5. Singlet spin-orbit potential $\delta V_{LS\ sb}$ in pNRQCD_{HTL}

In this section, we calculate the leading thermal corrections to the spin-orbit potential $\delta V_{LS\ sb}$, which is the spin-orbit potential experienced by the quarkonium when at rest with respect to the laboratory reference frame (we recall that, in our setup, this is also the reference frame of the thermal bath). This potential, even at zero temperature, is not constrained by Poincaré invariance.

In order to calculate $\delta V_{LS\ sb}$, we need to consider two new terms contributing to h_{so} in the pNRQCD Lagrangian: the term

$$-\frac{c_F}{4m} \boldsymbol{\sigma}^{(1)} \cdot r^i (\partial_i g\mathbf{B}), \quad (5.1)$$

and the term

$$\frac{c_s}{8m^2} \boldsymbol{\sigma}^{(1)} \cdot [\mathbf{p} \times, g\mathbf{E}], \quad (5.2)$$

where, for simplicity, we have put to their tree-level values the pNRQCD matching coefficients.

There are three classes of diagrams that contribute:

$$\delta V_{LS\ sb} = \delta V_{LS\ (i)} + \delta V_{LS\ (ii)} + \delta V_{LS\ (iii)}. \quad (5.3)$$

³We have explicitly checked that also the leading contribution to the spin-orbit potential, proportional to m_g^3/m^2 , satisfies the Gromes relation [33].

- (1) The first class is similar to the one shown in Fig. 2, but now the dots stand for insertions of the spin-orbit potential proportional to $V_{LS\,sb}$ (left and right diagram) or to $V_{LS\,ob}$ (middle diagram). $V_{LS\,sb}$ and $V_{LS\,ob}$ have been defined in Eqs. (2.7) and (2.8), and given at leading order in Eq. (2.9). The result reads

$$\delta V_{LS\,(i)}(r) = \frac{2\pi}{9} C_F \alpha_s T^2 r^2 (V_{LS\,ob}(r) - V_{LS\,sb}(r)) . \quad (5.4)$$

- (2) The second class is similar to the one shown in Fig. 3, but now the squares stand for the vertex induced by (5.1) and the cross for a kinetic energy insertion, \mathbf{p}^2/m . The result reads

$$\delta V_{LS\,(ii)}(r) = -\frac{4\pi}{9} C_F \alpha_s c_F T^2 \left(V_o^{(0)}(r) - V_s^{(0)}(r) \right) . \quad (5.5)$$

- (3) Finally, the third class of diagrams is similar to the ones evaluated in Sec. 3.2.3, but with the vertex proportional to $c_s V_{soa}^{(2,0)}$ in Eq. (2.15) replaced by the vertex induced by (5.2). The result reads

$$\delta V_{LS\,(iii)}(r) = \frac{2\pi}{9} C_F \alpha_s c_s T^2 \left(V_o^{(0)}(r) - V_s^{(0)}(r) \right) . \quad (5.6)$$

Summing up all three contributions we obtain

$$\begin{aligned} \delta V_{LS\,sb}(r) &= \frac{2\pi}{9} C_F \alpha_s T^2 \left[r^2 (V_{LS\,ob}(r) - V_{LS\,sb}(r)) - \left(V_o^{(0)}(r) - V_s^{(0)}(r) \right) \right] \\ &= -\frac{5\pi}{18} C_F N_c \frac{\alpha_s^2}{r} T^2 + \text{higher orders} , \end{aligned} \quad (5.7)$$

where, in the first equality, we have used that $2c_F - c_s - 1 = 0$.

6. Conclusions

We have calculated the leading-order thermal corrections to the quarkonium spin-orbit potentials. These corrections go quadratically with the temperature and are proportional to $\alpha_s^2 T^2/r$.

At zero temperature, the spin-orbit potential that depends on the centre-of-mass momentum is protected by Poincaré invariance. We have computed its leading thermal correction in Eq. (3.22). In Eq. (4.2), this correction has been shown to violate Poincaré invariance. This implies that order $\alpha_s^2 T^2/r$ corrections to the quarkonium potential will be experienced by the system differently in different reference frames, and, in particular, in a frame where the thermal bath is not at rest.

We have also computed the leading thermal correction to the spin-orbit potential of a quarkonium at rest with respect to the laboratory reference frame. Its expression is in Eq. (5.7). The potential contributes to the spin-orbit splittings of the quarkonium levels. The thermal correction being negative implies a weakening of the spin-orbit interaction in the medium.

In the special case of a bound state made of two heavy quarks with different masses, $m_1 \gg m_2$ (like the B_c system), the complete spin-dependent potential, up to corrections

of relative order m_2/m_1 , is given by $(V_{LS\ sa} + V_{LS\ sb})(\mathbf{r} \times \mathbf{p}_2) \cdot \boldsymbol{\sigma}_2/(4m_2^2)$. Therefore, the leading contribution to the hyperfine splittings reads

$$\delta E_{njl} = -\frac{\pi}{36} C_F^2 N_c \frac{\alpha_s^3}{m_2} T^2 \frac{j(j+1) - l(l+1) - 3/4}{n^2}, \quad (6.1)$$

where n , j and l are the principal, orbital and total angular momentum quantum numbers. The thermal correction has opposite sign with respect to the splitting at zero temperature, which implies smaller hyperfine splittings in the medium.

Acknowledgments

M.A.E. acknowledges useful discussions with Joan Soto in the early stages of this work. We acknowledge financial support from the DFG project BR4058/1-1 ‘‘Effective field theories for strong interactions with heavy quarks’’. N.B., J.G. and A.V. acknowledge financial support from the DFG cluster of excellence ‘‘Origin and structure of the universe’’ (www.universe-cluster.de). M.A.E. acknowledges financial support from the RTN Flavianet MRTN-CT-2006-035482 (EU) and the University of Milano for hospitality during the early stages of this work.

References

- [1] N. Brambilla, A. Pineda, J. Soto and A. Vairo, *Rev. Mod. Phys.* **77** (2005) 1423 [[arXiv:hep-ph/0410047](https://arxiv.org/abs/hep-ph/0410047)].
- [2] M. Laine, O. Philipsen, P. Romatschke and M. Tassler, *JHEP* **0703** (2007) 054 [[arXiv:hep-ph/0611300](https://arxiv.org/abs/hep-ph/0611300)].
- [3] M. Laine, *JHEP* **0705** (2007) 028 [[arXiv:0704.1720](https://arxiv.org/abs/hep-ph/0704.1720) [hep-ph]].
- [4] Y. Burnier, M. Laine and M. Vepsalainen, *JHEP* **0801** (2008) 043 [[arXiv:0711.1743](https://arxiv.org/abs/hep-ph/0711.1743) [hep-ph]].
- [5] N. Brambilla, J. Ghiglieri, A. Vairo and P. Petreczky, *Phys. Rev. D* **78** (2008) 014017 [[arXiv:0804.0993](https://arxiv.org/abs/hep-ph/0804.0993) [hep-ph]].
- [6] M. A. Escobedo and J. Soto, *Phys. Rev. A* **78** (2008) 032520 [[arXiv:0804.0691](https://arxiv.org/abs/hep-ph/0804.0691) [hep-ph]].
- [7] N. Brambilla, M. A. Escobedo, J. Ghiglieri, J. Soto and A. Vairo, *JHEP* **1009** (2010) 038 [[arXiv:1007.4156](https://arxiv.org/abs/hep-ph/1007.4156) [hep-ph]].
- [8] M. A. Escobedo and J. Soto, *Phys. Rev. A* **82** (2010) 042506 [[arXiv:1008.0254](https://arxiv.org/abs/hep-ph/1008.0254) [hep-ph]].
- [9] M. A. Escobedo, M. Mannarelli and J. Soto, [arXiv:1105.1249](https://arxiv.org/abs/hep-ph/1105.1249) [hep-ph].
- [10] T. Matsui and H. Satz, *Phys. Lett. B* **178** (1986) 416
- [11] N. Brambilla *et al.*, Heavy quarkonium physics, CERN-2005-005, (CERN, Geneva, 2005) [[arXiv:hep-ph/0412158](https://arxiv.org/abs/hep-ph/0412158)].
- [12] N. Brambilla *et al.*, *Eur. Phys. J. C* **71** (2011) 1534 [[arXiv:1010.5827](https://arxiv.org/abs/hep-ph/1010.5827) [hep-ph]].
- [13] A. Vairo, *AIP Conf. Proc.* **1317** (2011) 241 [[arXiv:1009.6137](https://arxiv.org/abs/hep-ph/1009.6137) [hep-ph]].
- [14] A. Pineda and J. Soto, *Nucl. Phys. Proc. Suppl.* **64** (1998) 428 [[arXiv:hep-ph/9707481](https://arxiv.org/abs/hep-ph/9707481)].

- [15] N. Brambilla, A. Pineda, J. Soto and A. Vairo, Nucl. Phys. B **566** (2000) 275 [arXiv:hep-ph/9907240].
- [16] M. E. Luke and A. V. Manohar, Phys. Lett. B **286** (1992) 348 [arXiv:hep-ph/9205228].
- [17] A. V. Manohar, Phys. Rev. D **56** (1997) 230 [arXiv:hep-ph/9701294].
- [18] N. Brambilla, D. Gromes and A. Vairo, Phys. Rev. D **64** (2001) 076010 [arXiv:hep-ph/0104068].
- [19] N. Brambilla, D. Gromes and A. Vairo, Phys. Lett. B **576** (2003) 314 [arXiv:hep-ph/0306107].
- [20] N. Brambilla, E. Mereghetti and A. Vairo, Phys. Rev. D **79** (2009) 074002 [arXiv:0810.2259 [hep-ph]].
- [21] D. Gromes, Z. Phys. C **26** (1984) 401.
- [22] A. Vairo, PoS **CONFINEMENT8** (2008) 002 [arXiv:0901.3495 [hep-ph]].
- [23] E. Braaten and R. D. Pisarski, Phys. Rev. D **45** (1992) 1827.
- [24] P. A. M. Dirac, Rev. Mod. Phys. **21** (1949) 392.
- [25] W. E. Caswell and G. P. Lepage, Phys. Lett. B **167** (1986) 437.
- [26] G. T. Bodwin, E. Braaten and G. P. Lepage, Phys. Rev. D **51** (1995) 1125 [Erratum-ibid. D **55** (1997) 5853].
- [27] A. V. Smirnov, V. A. Smirnov and M. Steinhauser, Phys. Rev. Lett. **104** (2010) 112002 [arXiv:0911.4742 [hep-ph]].
- [28] C. Anzai, Y. Kiyo and Y. Sumino, Phys. Rev. Lett. **104** (2010) 112003 [arXiv:0911.4335 [hep-ph]].
- [29] B. A. Kniehl, A. A. Penin, Y. Schröder, V. A. Smirnov and M. Steinhauser, Phys. Lett. B **607** (2005) 96 [arXiv:hep-ph/0412083].
- [30] N. Brambilla, A. Pineda, J. Soto and A. Vairo, Phys. Lett. B **470** (1999) 215 [arXiv:hep-ph/9910238].
- [31] N. Brambilla, X. Garcia i Tormo, J. Soto and A. Vairo, Phys. Lett. B **647** (2007) 185 [arXiv:hep-ph/0610143].
- [32] N. Brambilla, X. Garcia i Tormo, J. Soto and A. Vairo, Phys. Rev. D **80** (2009) 034016 [arXiv:0906.1390 [hep-ph]].
- [33] J. Ghiglieri, Ph.D. Thesis, TU Munich (2011).